Supplementary Information (SI) for Inorganic Chemistry Frontiers.

Tuning multifunctional stimuli-responsive behaviour through halogen exchange in hybrid ionic $[(CH_3CH_2)_3N(CH_2X)]_2[MnCl_4]$ (X = Cl, Br)

Javier García-Ben[a], María Gelpi[a], Pedro Dafonte-Rodríguez[a], Ángel Ferradanes-Martínez[a], Ignacio Delgado-Ferreiro[a], Jorge López-Beceiro[b], Ramón Artiaga[b], Antonio Luis Llamas-Saiz[c], Julian Walker[d], Charles James McMonagle[e], Alberto García-Fernández[a,f], Ute B Cappel[f,g], Socorro Castro-García[a], María Antonia Señarís-Rodríguez[a], Juan Manuel Bermúdez-García[a*], Manuel Sánchez-Andújar[a*]

[a] *University of A Coruna, QuiMolMat Group, Dpt. Chemistry, Faculty of Science and Centro Interdisciplinar de Química e Bioloxía (CICA), Zapateira, 15071 A Coruña, Spain. E-mail: j.bermudez@udc.es; m.andujar@udc.es*

[b] *CITENI-Proterm Group, Ferrol Industrial Campus, Campus de Esteiro, University of A Coruna, Ferrol, 15403 Spain.*

[c] *Research Infrastructures Area, X-ray Unit, University of Santiago de Compostela,15782 Santiago de Compostela, Spain.*

[d] *Norwegian University of Science and Technology, Department of Materials Science and Engineering, Trondheim 7491, Norway.*

[e] *European Synchrotron Radiation Facility, Swiss-Norwegian Beamlines, Grenoble 3843, France*

[f] *Division of X-ray Photon Science, Department of Physics and Astronomy, Uppsala University, Box 516, SE-751 20, Uppsala, Sweden.*

[g] *Wallenberg Initiative Materials Science for Sustainability, Department of Physics and Astronomy, Uppsala University, 751 20 Uppsala, Sweden.*

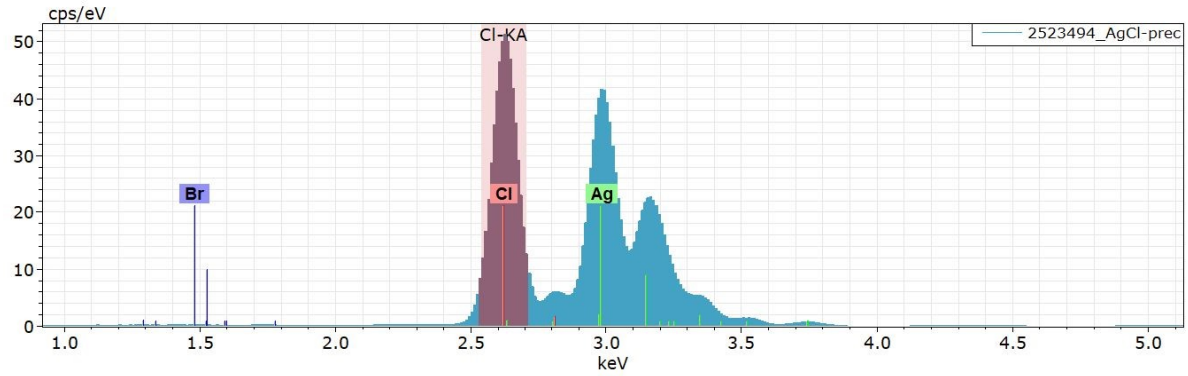

Figure S1. Micro X-ray fluorescence spectrum of the AgCl precipitate formed after $AgNO_3$ treatment of $[(CH_3CH_2)_3N(CH_2Br)]Cl$ in water, confirming successful Br^- to Cl^- anion exchange.

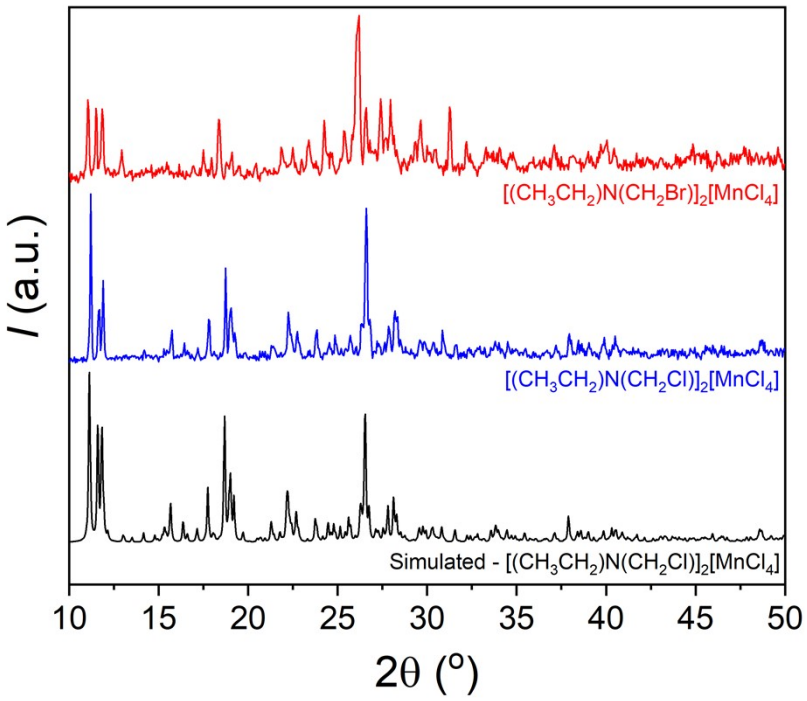

Figure S2. PXRD pattern at room temperature for $[(CH_3CH_2)_3N(CH_2Cl)]_2[MnCl_4]$ and $[(CH_3CH_2)_3N(CH_2Br)]_2[MnCl_4]$ compared with that simulated from the obtained SCXRD at 293 K.

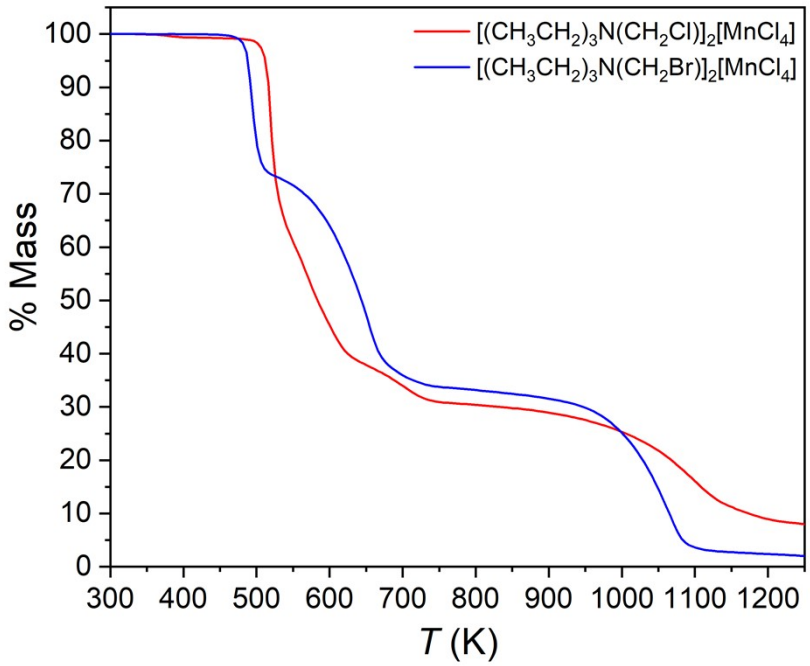

Figure S3. TGA decomposition curves of $[(CH_3CH_2)_3N(CH_2Cl)]_2[MnCl_4]$ and $[(CH_3CH_2)_3N(CH_2Br)]_2[MnCl_4]$ under N_2 atmosphere.

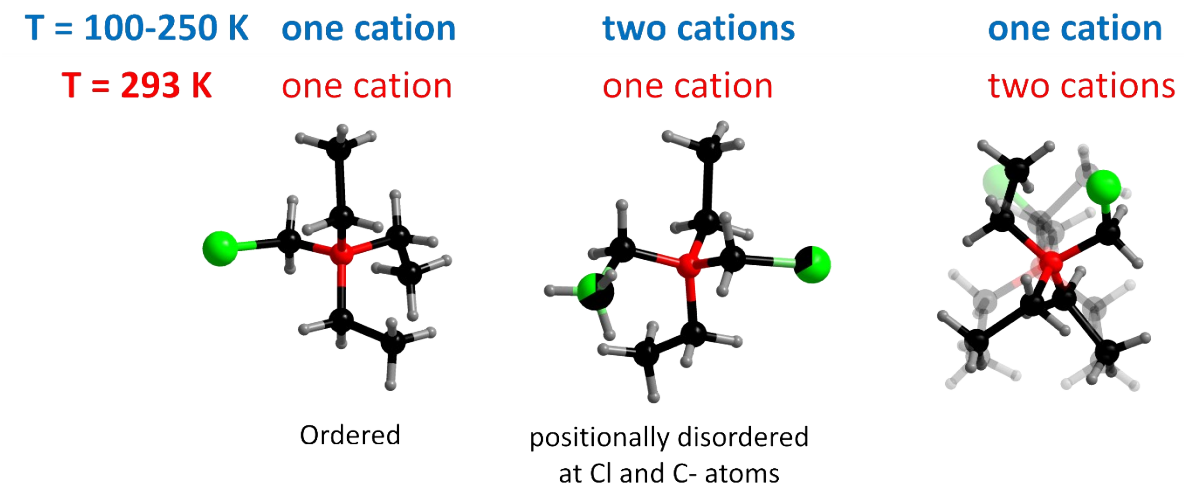

Figure S4. Observed configurations for the four $[(CH_3CH_2)_3N(CH_2Cl)]^+$ cations in the asymmetric unit at different temperatures between 100 K and 293 K.

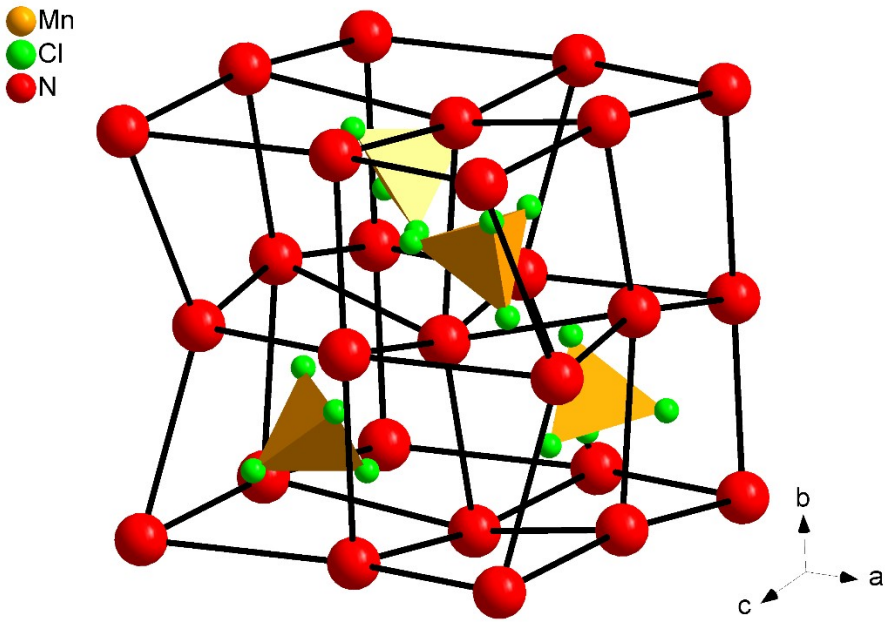

Figure S5. Coordination environment of $[MnCl_4]^{2-}$ anions showing the antifluorite structure.

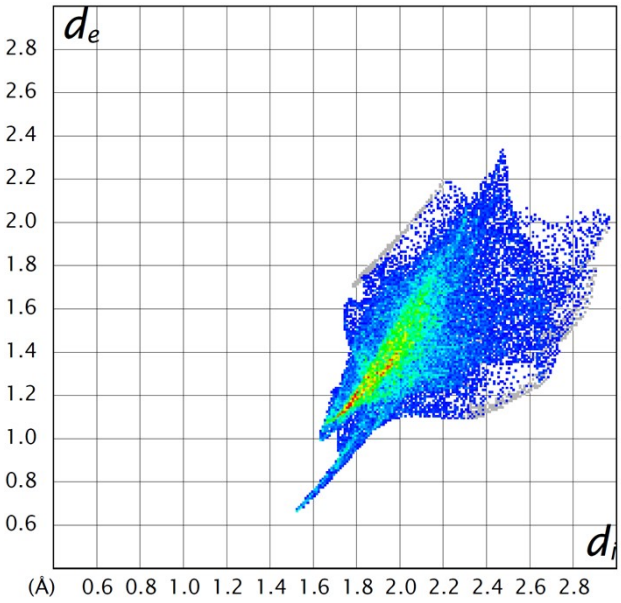

Figure S6. Fingerprint plot reveals close contacts between chloride atoms of the anion and hydrogen atoms of cations, encompassing approximately 97% of the Hirshfeld surface of $[MnCl_4]^{2-}$ anions.

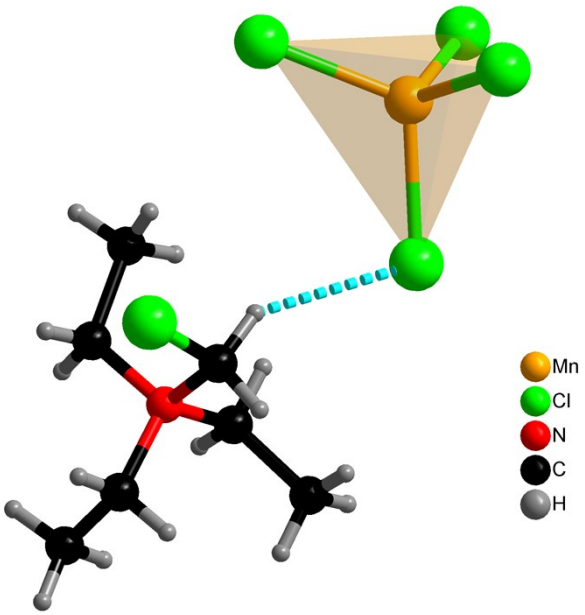

Figure S7. H-Cl interactions between the $[(CH_3CH_2)_3N(CH_2Cl)]^+$ cation and the $[MnCl_4]^{2-}$ anion.

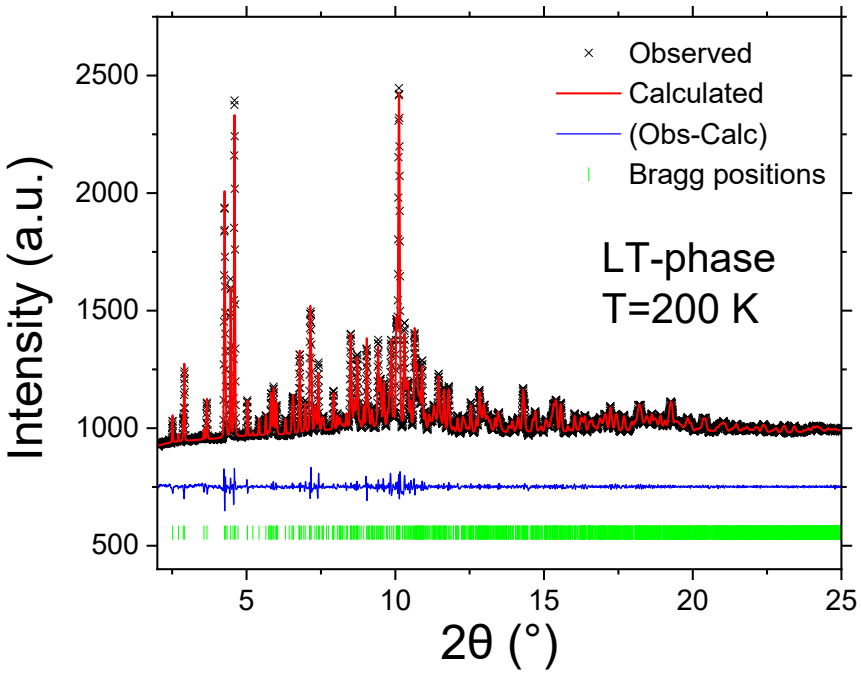

Figure S8. Le Bail refinement of LT-phase of $[(CH_3CH_2)_3N(CH_2Br)]_2[MnCl_4]$ at T = 200 K.

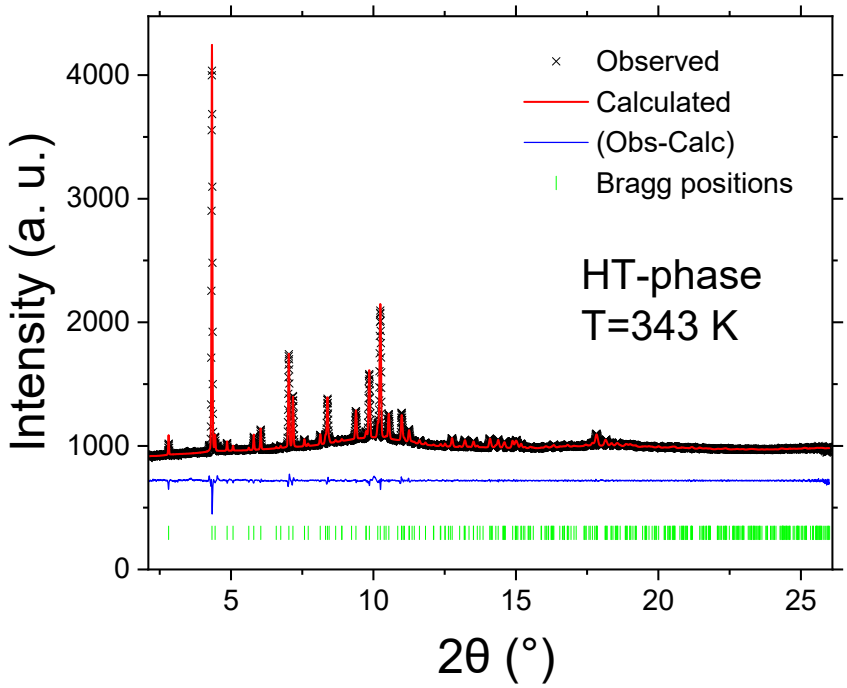

Figure S9. Le Bail refinement of HT-phase of $[(CH_3CH_2)_3N(CH_2Br)]_2[MnCl_4]$ at T = 343 K.

Table S1. Crystallographic data and structure refinement for $[(CH_3CH_2)_3N(CH_2Cl)]_2[MnCl_4]$ at different temperatures

	100 K	150 K	200 K	250 K	293 K	313 K	333 K
CCDC number	CCDC-2427812	CCDC-2427806	CCDC-2427811	CCDC-2427808	CCDC-2427807	CCDC-2427809	CCDC-2427810
Empirical formula	$C_{14}H_{34}N_2Cl_6Mn$	$C_{14}H_{34}N_2Cl_6Mn$	$C_{14}H_{34}N_2Cl_6Mn$	$C_{14}H_{34}N_2Cl_6Mn$	$C_{14}H_{34}N_2Cl_6Mn$	$C_{14}H_{34}N_2Cl_6Mn$	$C_{14}H_{34}N_2Cl_6Mn$
Formula weight	498.07 g/mol	498.07 g/mol	498.07 g/mol	498.07 g/mol	498.07 g/mol	498.07 g/mol	498.07 g/mol
Temperature	100.0 K	150.0 K	200.0 K	250.0 K	293.0 K	313.0 K	333.0 K
Crystal system	Triclinic	Triclinic	Triclinic	Triclinic	Triclinic	Tetragonal	Tetragonal
Space group	P-1	P-1	P-1	P-1	P-1	$P4_2/nmc$	$P4_2/nmc$
a	12.9343(6) Å	12.9670(6) Å	13.0014(5) Å	13.0388(4) Å	13.0955(3) Å	9.1302(5) Å	9.1803(4) Å
b	13.4694(6) Å	13.5011(6) Å	13.5279(5) Å	13.5536(4) Å	13.5645(4) Å	9.1302(5) Å	9.1803(4) Å
c	15.8152(6) Å	15.8509(7) Å	15.9079(5) Å	15.9615(4) Å	16.0265(5) Å	14.7396(12) Å	14.6746(10) Å
α	110.2319(15)°	110.3266(14)°	110.3856(12)°	110.3794(10)°	110.5087(11)°	90°	90°
β	113.3974(15)°	113.3961(14)°	113.3517(9)°	113.1963(7)°	113.0449(10)°	90°	90°
γ	90.7442(17)°	90.7111(16)°	90.7295(10)°	90.8769(8)°	90.9333(10)°	90°	90°
Volume	2336.27(18) $Å^3$	2351.52(19) $Å^3$	2370.59(15) $Å^3$	2392.09(12) $Å^3$	2414.43(12) $Å^3$	1228.70(17) $Å^3$	1236.74(14) $Å^3$
Z	4	4	4	4	4	2	2
ρ_{calc}	1.416 g/cm^3	1.407 g/cm^3	1.396 g/cm^3	1.383 g/cm^3	1.370 g/cm^3	1.346 g/cm^3	1.337 g/cm^3
μ/mm^{-1}	1.251 mm^{-1}	1.243 mm^{-1}	1.233 mm^{-1}	1.222 mm^{-1}	1.211 mm^{-1}	1.19 mm^{-1}	1.182 mm^{-1}
F(000)	1036	1036	1036	1036	1036	518	518
Crystal size/mm^3	0.29 × 0.149 × 0.085	0.29 × 0.149 × 0.085	0.29 × 0.149 × 0.085	0.29 × 0.149 × 0.085	0.595 × 0.565 × 0.128	0.595 × 0.565 × 0.128	0.595 × 0.565 × 0.128
Radiation	MoKα (λ = 0.71073)	MoKα (λ = 0.71073)	MoKα (λ = 0.71073)	MoKα (λ = 0.71073)	MoKα (λ = 0.71073)	MoKα (λ = 0.71073)	MoKα (λ = 0.71073)
2Θ range for data collection	4.344 to 72.738°	4.334 to 56.614°	4.324 to 52.786°	4.308 to 52.764°	4.292 to 56.726°	5.528 to 50.074°	6.276 to 50.074°
Index ranges	-21 ≤ h ≤ 21 -22 ≤ k ≤ 22 -23 ≤ l ≤ 26	-17 ≤ h ≤ 17 -17 ≤ k ≤ 17 -21 ≤ l ≤ 21	-16 ≤ h ≤ 16 -16 ≤ k ≤ 16 -19 ≤ l ≤ 19	-16 ≤ h ≤ 16 -16 ≤ k ≤ 16 -19 ≤ l ≤ 19	-16 ≤ h ≤ 17 -18 ≤ k ≤ 18 -21 ≤ l ≤ 21	-10 ≤ h ≤ 10 -10 ≤ k ≤ 10 -17 ≤ l ≤ 17	-10 ≤ h ≤ 10 -10 ≤ k ≤ 10 -17 ≤ l ≤ 17
Reflections collected	204116	37844	32708	32919	82052	6697	13500
Independent reflections	22139 [R_{int} = 0.0475, R_{sigma} = 0.0301]	10827 [R_{int} = 0.0583, R_{sigma} = 0.0531]	9095 [R_{int} = 0.0552, R_{sigma} = 0.0471]	9157 [Rint = 0.0494, Rsigma = 0.0416]	12059 [R_{int} = 0.0333, R_{sigma} = 0.0190]	616 [Rint = 0.0485, Rsigma = 0.0219]	621 [R_{int} = 0.0393, R_{sigma} = 0.0149]
Data/restraints/parameters	22139/410/515	10827/410/515	9095/410/515	9157/410/515	12059/952/599	616/116/88	621/116/88
Goodness-of-fit on F^2	1.030	1.028	1.029	1.024	1.020	1.150	1.391
Final R indexes [I>=2σ (I)]	R_1 = 0.0361 wR_2 = 0.0832	R_1 = 0.0400 wR_2 = 0.0878	R_1 = 0.0407 wR_2 = 0.0938	R_1 = 0.0482 wR_2 = 0.1269	R_1 = 0.0564 wR_2 = 0.1728	R_1 = 0.0793 wR_2 = 0.2644	R_1 = 0.0743 wR_2 = 0.2780
Final R indexes [all data]	R_1 = 0.0548, wR_2 = 0.0920	R_1 = 0.0654, wR_2 = 0.0979	R_1 = 0.0645, wR_2 = 0.1045	R1 = 0.0720, wR2 = 0.1426	R_1 = 0.0699, wR_2 = 0.1877	R_1 = 0.0927, wR_2 = 0.2815	R_1 = 0.0819, wR_2 = 0.2975
Largest diff. peak/hole	1.34/-1.16 e $Å^{-3}$	0.58/-0.53 e $Å^{-3}$	0.41/-0.50 e $Å^{-3}$	0.62/-0.59 e $Å^{-3}$	0.93/-0.98 e $Å^{-3}$	0.48/-0.39 e $Å^{-3}$	0.44/-0.50 e $Å^{-3}$

Table S2. Bond lenghts of the $[MnCl_4]^-$ anions for $[(CH_3CH_2)_3N(CH_2Cl)]_2[MnCl_4]$ at different temperatures

Mn – Cl bonds								
Atom	**Atom**	**Length (Å)**						
		100 K	**150 K**	**200 K**	**250 K**	**293 K**	**313 K**	**333 K**
Mn(1)	Cl(1)	2.3737(4)	2.3710(8)	2.3699(9)	2.3677(11)	2.3676(10)	2.336(2)	2.336(2)
Mn(1)	Cl(2)	2.3884(4)	2.3880(8)	2.3876(9)	2.3891(11)	2.3904(10)		
Mn(1)	Cl(3)	2.3784(4)	2.3755(8)	2.3757(9)	2.3730(12)	2.3679(10)		
Mn(1)	Cl(4)	2.3574(4)	2.3550(9)	2.3529(10)	2.3505(13)	2.3464(12)		
Mn(2)	Cl(21)	2.3716(4)	2.3703(7)	2.3688(9)	2.3668(10)	2.3609(9)		
Mn(2)	Cl(22)	2.3501(4)	2.3492(7)	2.3475(8)	2.3452(10)	2.3402(9)		
Mn(2)	Cl(23)	2.3568(4)	2.3534(7)	2.3542(8)	2.3532(10)	2.3549(9)		
Mn(2)	Cl(24)	2.3704(4)	2.3683(7)	2.3662(9)	2.3629(11)	2.3589(9)		

Table S3. Bond angles of the $[MnCl_4]^-$ anions for $[(CH_3CH_2)_3N(CH_2Cl)]_2[MnCl_4]$ at different temperatures

Mn – Cl bonds									
Atom	**Atom**	**Atom**	**Angle (º)**						
			100 K	**150 K**	**200 K**	**250 K**	**293 K**	**313 K**	**333 K**
Cl(1)	Mn(1)	Cl(2)	102.242(13)	102.45(3)	102.73(3)	103.02(4)	103.02(4)	109.13(8)	108.92(7)
Cl(1)	Mn(1)	Cl(3)	114.815(14)	114.75(3)	114.64(4)	114.34(5)	113.75(4)	110.15(15)	110.59(13)
Cl(3)	Mn(1)	Cl(2)	109.700(14)	109.56(3)	109.44(3)	109.03(4)	108.89(4)		
Cl(4)	Mn(1)	Cl(1)	107.609(15)	107.49(3)	107.51(4)	107.73(5)	108.07(5)		
Cl(4)	Mn(1)	Cl(2)	115.153(17)	115.02(4)	114.83(4)	114.61(6)	114.73(6)		
Cl(4)	Mn(1)	Cl(3)	107.489(17)	107.71(3)	107.84(4)	108.22(5)	108.45(6)		
Cl(22)	Mn(2)	Cl(21)	109.856(14)	109.90(3)	109.98(3)	109.96(4)	110.11(4)		
Cl(22)	Mn(2)	Cl(23)	106.212(14)	106.29(3)	106.38(3)	106.54(4)	106.76(4)		
Cl(22)	Mn(2)	Cl(24)	108.858(14)	108.82(3)	108.91(3)	109.17(4)	109.29(4)		
Cl(23)	Mn(2)	Cl(21)	111.698(14)	111.66(3)	111.61(3)	111.35(4)	111.10(4)		
Cl(23)	Mn(2)	Cl(24)	107.984(13)	108.12(3)	108.24(3)	108.50(4)	108.71(4)		
Cl(24)	Mn(2)	Cl(21)	112.023(14)	111.85(3	111.55(3)	111.19(4)	110.77(4)		